Atmospheric Environment 190 (2018) 116–125

Contents lists available at ScienceDirect

Atmospheric Environment

journal homepage: www.elsevier.com/locate/atmosenv

Field measurements of solid-fuel cookstove emissions from uncontrolled cooking in China, Honduras, Uganda, and India

S. Rose Eilenberg[a], Kelsey R. Bilsback[b], Michael Johnson[c], John K. Kodros[d], Eric M. Lipsky[a,e], Agnes Naluwagga[f], Kristen M. Fedak[g], Megan Benka-Coker[g], Brooke Reynolds[g], Jennifer Peel[g], Maggie Clark[g], Ming Shan[h], Sankar Sambandam[i], Christian L'Orange[b], Jeffrey R. Pierce[d], R. Subramanian[a], John Volckens[b], Allen L. Robinson[a,*]

[a] Department of Mechanical Engineering, Carnegie Mellon University, 500 Forbes Ave Pittsburg, Pennsylvania, 15213, United States
[b] Department of Mechanical Engineering, Colorado State University, 1374 Campus Delivery, Fort Collins, CO, 80523, United States
[c] Berkeley Air Monitoring Group, 1900 Addison St. Suite 350, Berkeley, CA, United States
[d] Department of Atmospheric Science, Colorado State University, 1371, Campus Delivery, Fort Collins, CO, United States
[e] Department of Mechanical Engineering, Penn State Greater Allegheny, 4000 University Drive, McKeesport, Pennsylvania, 15132, United States
[f] Centre for Research in Energy and Energy Conservation (CREEC), Uganda
[g] Department of Environmental & Radiological Health Sciences, Colorado State University, Fort Collins, CO, United States
[h] Department of Building Science, School of Architecture, Tsinghua University, Beijing, China
[i] Department of Environmental Health Engineering, Faculty of Public Health, Sri Ramachandra Medical College and Research Institute, Chennai, India

ARTICLE INFO

Keywords:
Particulate matter
Cookstoves
Household energy
Biomass
Climate change
Residential emissions
Solid fuel

ABSTRACT

Cookstoves have wide-reaching impacts on human health, air quality, and the climate. We measured emissions from uncontrolled cooking in 41 households in China, Honduras, Uganda, and India using a portable sampler. Test sites were chosen to cover a range of stove types (traditional and "improved"), fuels (wood, charcoal and coal), and cooking practices. We report test-integrated fuel-based emission factors (EFs) of fine particulate matter ($PM_{2.5}$) mass, organic carbon (OC), elemental carbon (EC), as well as real time EFs of carbon monoxide (CO), black carbon (BC), total particle number, and particle size distributions. There was substantial house-to-house variability in emissions; the distribution of EFs were also highly positively skewed by several "super-emitter" stoves in China (those with $PM_{2.5}$ EFs 5–20 times greater than the median value). The highest $PM_{2.5}$ mass emission factors were measured in China (median:10.3 g/kg-fuel), and the lowest in Uganda (median: 1.7 g/kg-fuel). The median $PM_{2.5}$ mass EFs in wood-burning stoves in Honduras and India were similar: 3.7 g/kg-fuel and 4.1 g/kg-fuel, respectively. However, Indian stoves had higher EC EFs then Honduran stoves, demonstrating that emissions depend on more that fuel type; regional differences, such as cooking styles and stove design, may influence aerosol properties as well. Coal and charcoal stoves had higher OC:EC than wood stoves. The differences between the CO, $PM_{2.5}$, and OC:EC ratios of "improved" and traditional stoves in India and Honduras were not statistically significant. To the best of our knowledge, we report the first cookstove source size distributions measurements from uncontrolled in-home cooking. These distributions varied between countries, which will influence local radiative effects. Particle size distributions from stoves tested in China, Honduras, and India were unimodal in the size range measured, with geometric mean diameters (GMDs) of 66 nm, 48 nm, and 76 nm, respectively. The median GMD of particles emitted from Ugandan charcoal stoves was 39, and when all tests are averaged, the resulting distribution appears tri-modal, with modes near 15, 30, and 100 nm. Real-time emissions data reveal high BC and particle number emissions during startup and fuel additions, which can be seen in the positively skewed distributions. Emissions of BC were most skewed, indicating that they were highly event-driven, followed by total particle number. CO emissions were more evenly spread across cooking events.

* Corresponding author.
E-mail address: alr@andrew.cmu.edu (A.L. Robinson).

https://doi.org/10.1016/j.atmosenv.2018.06.041
Received 14 March 2018; Received in revised form 22 June 2018; Accepted 25 June 2018
Available online 28 June 2018

1. Introduction

More than 3 billion people depend on solid fuel-burning stoves for cooking and heating (World Health Organization, 2018). Biofuel combustion contributes roughly 20% of global black carbon (BC) and organic carbon (OC) emissions (Bond et al., 2004). Exposure to indoor air pollution from solid-fuel combustion is a major contributor to morbidity and mortality in the developing world (Ezzati and Kammen, 2001) and is estimated to be responsible for the premature deaths of between 2 and 4 million people each year (World Health Organization, 2018; Kodros et al., 2018). In addition to the associated health risks, PM emissions from stoves influence the climate through both direct (scattering and/or absorbing solar radiation) and indirect (changing the radiative properties of clouds) effects. Currently, the net aerosol-climate effects of cookstove technology are uncertain, with reported climate forcing ranging from net warming to net cooling (Kodros et al., 2015; Koch et al., 2007; Lacey and Henze, 2015). For example, Lacey and Henze (2015) estimate that removing all cookstove emissions could result in a range of 0.16 K warming to 0.28 K cooling. Critical emission uncertainties include the emission rates, the composition of co-emitted species, particle mixing state, and particle size distributions.

Stove emissions are often characterized by laboratory testing. However, this testing may not represent real-world emissions (Roden et al., 2009; Wathore et al., 2017). For example, previous studies have found that PM emissions measured in the field are two to three times higher than those measured on the same stove technology in the laboratory, with considerably more variation (Roden et al., 2009). Emissions depend on stove design, fuel type, and cooking practices. Laboratory tests often use highly-prescribed test protocols, such as the Water Boiling Test (WBT). While these prescribed protocols facilitate direct comparison of different stove designs, they do not necessarily reflect real-world stove use patterns (Bailis et al., 2007). In addition, stove operation can vary widely by region: for example, we observed in some regions users add fuel sporadically over many hours, while others fill the stove to capacity for shorter, more intense cooking sessions. Laboratory tests often use carefully prepared fuels, which may not be representative of the wide array of fuel size, composition, and moisture content found in the field (Bhattacharya et al., 2002).

There have been a number of studies reporting uncontrolled in-home emissions of stoves in India (Grieshop et al., 2017), Uganda (Johnson et al., 2011; Adkins, 2010), Ghana (Coffey et al., 2017), China (Chen X. L., 2015; Wei et al., 2014; Zhang et al., 2008), Honduras (Roden et al., 2006; Roden et al., 2009), and Mexico (Johnson et al., 2008). Comparisons of emissions between regions can be difficult because studies report emissions of different pollutants and evaluate performance using different metrics (fuel or energy based emission factors (EFs), indoor concentrations, or fuel efficiency), and measurements were made using different instrumentation. Few studies measure continuous emissions (Roden et al., 2009; Chen Y. R., 2012), which can identify specific operations leading to high emission events. Many studies that do measure real-time data only report pollutant concentrations in the kitchen, not emission factors (Masera et al., 2007; Kar et al., 2012; Dutta et al., 2007; Leavey, 2015; Ezzati et al., 2000). Finally, there are gaps in the existing data from field studies; for example, we are not aware of uncontrolled, in-home measurements of source particle size distributions. Particle size distributions are a critical input for understanding the climate effects from cookstove emissions (Kodros et al., 2015). For the same mass emissions, smaller and narrower size distributions reduce the direct radiative effect (DRE), while decreasing the mean diameter increases the scattering through the aerosol indirect effect (AIE) (Kodros et al., 2015). Therefore, regional variability in emissions size distributions will change the spatial distribution of radiative effects relative to previous estimates.

Real-world stove emissions are critical inputs for both climate and air quality models, as well a baseline for large-scale cookstove interventions. In this paper, we report and compare emissions from in-home cookstoves in 41 different households across four countries: China, Honduras, Uganda, and India. These sites were chosen to build a dataset which represents a range of stove technologies, including traditional and "improved" stoves (i.e. stoves that have some modification to their combustion chamber to improve thermal efficiency), as well as a variety of fuels and cooking practices. We measured emissions of a suite of pollutants using the same instruments and protocols at each field site. We report data as fuel-based emission factors calculated using the carbon balance method and compare our results to published data.

2. Methods

2.1. Stoves

Tests were conducted at sites in China, Honduras, Uganda, and India. The stove-fuel combinations were selected to be indicative of large geographic regions with different stove-fuel use patterns, with the intent of providing baseline data for global and regional models. Local partners in each country assisted in identifying appropriate testing houses to cover a representative range of primarily traditional and some "improved" stoves. For a household to be eligible, they had to rely primarily on biomass and/or coal for their cooking and heating, be logistically accessible, and not be in close proximity to a major source of emissions such as a large highway or power plant. The stoves were required to be operated by the primary cook for the household. Institutional Review Board approval was granted by Colorado State University and all participants were recruited using informed consent.

We measured emissions during uncontrolled usage events, lasting from just under 1 h to over 7 h. The cooks from each household were asked to operate their stove as they normally would, so we could measure emissions during typical use, including stove operation practices that might not be captured in laboratory experiments. Stoves in China and Honduras were typically operated continuously throughout the day, meaning startup and shutdown events were not as relevant to daily use, while in India and Uganda, startup and shutdown were distinct events.

Table 1 provides a brief overview of the tests conducted, including stove/fuel combinations. In China, we tested seven coal chimney stoves, one open coal stove, one traditional chimney wood stove, and two chimney biomass pellet-burning stoves. These stoves were primarily used for space heating.

In Honduras, we tested five traditional built-in wood-burning plancha stoves and five "improved" plancha stoves. Plancha stoves are designed to totally enclose the fire, and direct the hot flue gases to a flat cooking surface. The combustion chamber of the improved plancha stoves were built in the enclosed "rocket" style, featuring insulated, L-shaped combustion chambers to improve combustion efficiency and increase heat transfer to cooking vessels. The most common cooking

Table 1
Overview of tests performed.

Country	Fuel Type	N_{total}	N_{Imp}	Common Tasks	Avg. Test Length (hrs)
China	Coal: unprocessed (n = 3) Coal: honeycomb briquettes (n = 5) biomass pellets (n = 2) wood (n = 1)	11	2	Space Heating/ Boiling water	4.7 ± 2
Honduras	Wood	10	5	Beans, tortillas	3.6 ± 0.4
Uganda	Charcoal (n = 9) Wood (n = 1)	10	2	Porridge, rice, vegetables, boiling water	2.7 ± 0.5
India	Wood	10	3	Vegetable stews and rice	1.3 ± 0.3

tasks in Honduras were preparing beans and tortillas. In Uganda, we tested eight traditional and two locally made "improved" charcoal stoves as well as one three-stone-fire. In Uganda, cooks made porridge, rice, and vegetables. In India, we tested seven traditional stoves: five built-in mud chulhas and two ceramic rocket-elbow stoves used to make rice and vegetable stew. We also tested three insulated rocket-elbow stoves. Photographs of a typical stove from each country can be found in the supporting information (SI) (S5-S8).

Performance of "improved" stoves were compared in two countries, Honduras and India, due to the use of a common fuel. For this study, we did not set a minimum performance tier (e.g. as defined by the 2012 Global Alliance for Clean Cookstoves, "IWA Tiers of Performance" (Global Alliance for Clean Cookstoves, 2012)), but define an "improved" stove as one that had been distributed into the community by local stove programs and has some modification to the combustion chamber to improve combustion or thermal efficiency. In Honduras, these were "improved" plancha stoves, developed by Trees, Water, and People; Rotary International; and the Aprovecho Research Center, in partnership with local people. In India we defined the locally produced Envirofit "SuperSaver AI Wood", a rocket stove, as "improved".

2.2. Experimental setup

2.2.1. Instrumentation

We used a battery-powered portable emissions sampler (Fig. S1) to characterize cookstove emissions. The sampler was based on the design of Wathore et al. (Wathore et al., 2017). The sampler consisted of a 6-armed stainless-steel probe with multiple holes along the length of each arm, which was placed 1–1.5 m over the stove, or at the exit of the chimney (if present). This design allowed for representative sampling of the emissions plume. The position of the probe was adjusted to maintain a target CO_2 concentration through the natural dilution of the plume that was substantially above background (~2000 ppm). The exhaust sample was passed through a cyclone with a 2.5 μm cut point and then was split passing through two filter cartridges in parallel and real-time instruments.

Real time concentrations of CO_2 and CO were measured using an AQ Expert portable indoor air quality monitor (E instruments, Langhorne, PA. Sensor types— CO_2: NDIR; CO: electrochemical). The gas monitor was calibrated before and after sampling trips to each country. Continuous particle measurements included size distributions in 13 bins from 10 nm to 420 nm (NanoScan SMPS Nanoparticle Sizer, Model 3910; TSI, Shoreview, MN) and black carbon concentrations (microAeth Model AE51; AethLabs, San Francisco, CA). The NanoScan and microAeth sampling lines each had optional dilution air which was used during periods of high particle concentrations. Filtered dilution air was drawn from outside the testing house; when chimneys were present, the dilution line was placed on the opposite side of the house.

2.2.2. Aethalometer corrections

Two post-processing algorithms were applied to the microAeth data. The Optimized Noise-reduction Averaging algorithm (Hagler et al., 2011) adjusts averaging times to account for high signal-to-noise ratios at low concentrations. Filter tabs were changed per the manufacturer's specifications, when the instrument signaled it was necessary (at an attenuation of 125); we corrected for effects of filter loading using the approach of Kirchstetter and Novakov (2007), in which the mass-specific attenuation coefficient is defined as a function of filter transmission at each measurement point, instead of remaining constant (Kirchstetter and Novakov, 2007).

2.2.3. Filter analysis

To characterize $PM_{2.5}$ mass and composition, integrated filter samples were collected over the entire duration of each test. Two parallel sets of filter cartridges were collected. One contained a single quartz filter (Tissuquartz; Pall Corporation, Port Washington, NY), which was used to measure organic and elemental carbon. Because gaseous organic material will adsorb onto quartz filters, filter-based OC measurements are prone to positive artifacts. To correct for these artifacts, a second quartz filter was placed behind a Teflon filter (QBT-quartz behind Teflon (Subramanian et al., 2004)). The Teflon filter (Fiberfilm; Pall Corporation; Port Washington, NY) collects all the $PM_{2.5}$ mass, which was determined gravimetrically. The OC measured on the QBT is a measure of the adsorbed organic gases; it was subtracted from the bare quartz to account for this artifact. Negative artifacts are assumed to be negligible (Subramanian et al., 2004).

Teflon filters were weighed pre- and post-test after 24 h of conditioning in a temperature and relative humidity controlled environment to determine gravimetric $PM_{2.5}$ mass. Quartz filters were analyzed using thermal-optical analyzer (TOA; Sunset Laboratory, Tigard, OR) using the IMPROVE_A protocol (Chow et al., 2007). The organic carbon measured on the QBT filters was subtracted from that measured on the bare quartz filter to estimate particulate organic carbon (Subramanian et al., 2004). We used an organic-matter-to-organic-carbon (OM:OC) ratio of 1.9 for wood and 1.33 for coal and charcoal to estimate the primary organic aerosol (POA) based on the measured OC ($POA = \left[{}^{OM}/_{OC}\right] * OC$). The 1.33 value for coal and charcoal was found by Hu et al. (2013) for coal combustion aerosol in China. The 1.9 value for wood, used by Roden et al. (2006), Coffey et al. (2017), and MacCarty et al. (2008), is based on results from fireplace combustion of pine and oak (Turpin and Lim, 2001).

Quartz filters were pre-baked in air to remove any residual carbon. Clean handling procedures were used to minimize filter contamination. Quality assurance procedures for integrated samples include characterization of field blanks and replicate analyses. The mass on field blanks, which were collected during each test, were 0.3% and 0.1% of the average mass for test quartz and Teflon filters, respectively.

2.3. Fuel-based emission factors

The measured pollutant concentrations were converted to fuel-based emission factors using the carbon balance method, assuming all the carbon in the fuel is converted to CO and CO_2. The emission factor, EF, is given by:

$$EF\left({}^{g}/_{kg-fuel}\right) = \frac{\Delta[pollutant]}{\Delta CO + \Delta CO_2} * Fuel\ Carbon\ Content$$

Where $\Delta[pollutant]$ is the background-corrected pollutant concentration, and $\Delta CO + \Delta CO_2$ is the sum of background-corrected concentrations of CO and CO_2. Some fuel carbon is emitted as other species; prior work suggests these species introduce an error of 1–4% in cookstove experiments (Roden et al., 2006). Fuel samples collected from field sites were analyzed to determine the fuel carbon content (kg-C/kg-fuel). Pre- and post-test background levels of CO and CO_2 were low relative to the emissions: the average CO background subtraction was 1.4%, and the average CO_2 background subtraction was stable, with an average of 26.7%. Indoor concentrations of the measured pollutants can increase to non-negligible percentages of plume concentrations during stove operation (Leavey, 2015), though they quickly return to background levels after the test, due to natural ventilation. For stoves without chimneys, this means that some of the indoor air with elevated concentrations will be entrained in the plume. The concentrations of co-emitted species will increase together, and will, therefore, be accounted for with the carbon balance method used to calculate emission factors. However, there is likely a few minute lag in the background concentrations relative to the instantaneous emissions.

Filter-based EFs were calculated using the total measured mass (either gravimetrically or with TOA) and the average background-corrected CO + CO_2 concentrations over the sampling period. We did not collect filter measurements of background $PM_{2.5}$ concentrations. However, given the high $PM_{2.5}$ concentrations in the stove exhaust,

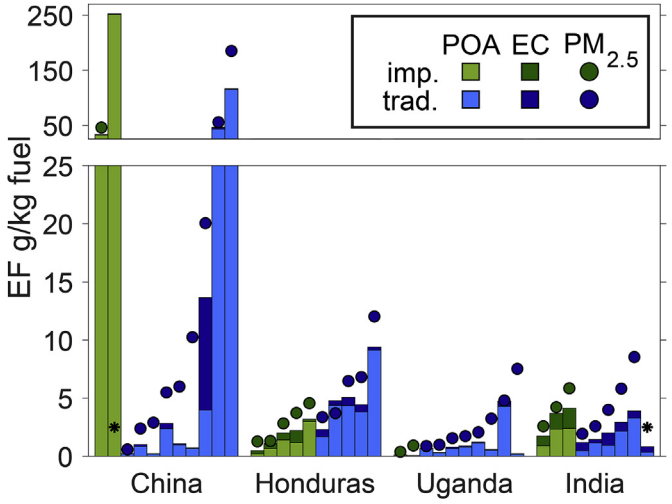

Fig. 1. Test-average filter-based fine particulate matter (PM2.5) emission factors (EFs) from all tests. Data are grouped by country; within each country, the "improved" stoves (green bars) and the traditional stoves (blue bars) are presented in rank order of gravimetric PM2.5 emission factors. For each bar, the lighter colored area on the bottom represents (artifact-corrected) primary organic aerosol (POA) and the darker section on top represents EC emissions. Filled circles represent the total PM2.5 emission factors from gravimetric measurements. Asterisks indicate tests missing total PM2.5 EFs due to compromised filter data.

only extremely high background concentrations would create any appreciable bias. For example, background $PM_{2.5}$ mass concentrations of 40 and 200 μg/m^3 would only contribute 1% and 5% of the average filter loading, respectively. One-minute average EFs were calculated for CO, BC, and particle size distribution data. Finally, we calculated the modified combustion efficiency (MCE), using the following formulation:

$$MCE = \frac{\Delta CO_2}{\Delta CO + \Delta CO_2}$$

3. Results and discussion

3.1. Test integrated emissions

The gravimetric $PM_{2.5}$ mass and carbonaceous $PM_{2.5}$ emission factors for all tests, grouped by both country and stove type (traditional or "improved") are given in Fig. 1. These are test-integrated measurements, including startup and shutdown in countries where these distinct events occurred. The complete set of test-integrated data are tabulated in Table S1.

There was substantial household-to-household variability in PM EFs., with measurements ranging from 0.4 g/kg-fuel to 185 g/kg-fuel. The data are positively skewed, meaning that averages (e.g. country-wide) are sensitive to several high emitters. The datasets collected here are likely too small to define robust country-wide average emissions factors. Therefore, we report the median values and interquartile ranges (IQR) of the data instead of arithmetic means.

The gravimetric $PM_{2.5}$ mass EFs had a median of 3.7 g/kg-fuel across all tests, and an IQR of 4.4 g/kg-fuel. The median POA EF was 1.1 g/kg-fuel with an IQR of 2.8 g/kg-fuel. There were, however, several tests with considerably higher POA EFs in China. EC EFs were lower on-average than POA, though also varied widely, with a median of 0.44 g/kg-fuel and an IQR of 0.7 g/kg-fuel.

Figure S2 indicates that for most tests, carbonaceous aerosols (POA + EC) contributed the majority of the $PM_{2.5}$. The median ratio of POA + EC to total $PM_{2.5}$ mass was 0.6, with an IQR of 0.3. There was reasonable correlation between the $PM_{2.5}$ EF vs carbonaceous aerosol EF, with a slope of 0.59 and an R^2 of 0.7 (when not including EFs over 45). However, for three tests of coal-burning stoves in China and three tests of charcoal-burning stoves in Uganda, the carbonaceous material contributed much less than half of the $PM_{2.5}$ mass. There are several potential explanations: we assumed a constant OM:OC ratio for each test, but it can be higher at certain operating conditions, such as smoldering. Another possible contributor is inorganics, which are present in higher quantities in charcoal and coal fuels (Spliethoff, 2010).

The test-average $PM_{2.5}$ mass EFs are grouped by country in Fig. 2a. Emissions depend on many factors, including stove design, fuel type and conditions, and user operation, all of which vary widely between regions. For example, all of our coal data are from China, the wood data are from Honduras and India, and the charcoal data are from Uganda. Garbage and food waste was used as fuel sporadically in Honduras, while dung was sometimes used in India. Cooking tasks also varied by country. The primary applications were: space heating in China, boiling or stewing in Uganda, tortilla preparation in Honduras, and rapid frying and stewing in India. Because it is impossible to isolate the effects of each individual factor with a sample this size, we focus on comparing country-level data.

Stoves in China had the highest $PM_{2.5}$ mass emissions, particularly those burning unprocessed coal and biomass pellets. In China, the median $PM_{2.5}$ mass EF was 8.1 g/kg-fuel (interquartile range: 35.9 g/kg-fuel). The highest $PM_{2.5}$ emissions (> 100 g/kg-fuel) were from two tests in China: one burning unprocessed coal and the other biomass pellets. These values are much higher than previously reported emission factors (Zhang et al., 2000; Zhang et al., 2008; Shen et al., 2015). (See Fig. S3 for a photograph of one such test). Multiple, independent measurements indicate that these high emissions are not an error. For example, for one of these two tests the quartz and Teflon filter EFs agree to within 12%, and for the second (POA + EC = 252 g/kg-fuel) the Teflon filter couldn't be weighed due to an experimental issue. Additionally, the geometric mean diameter (GMD) of the particle number size distributions from these two tests were 139 and 114 nm, much greater than other tests. While the $PM_{2.5}$ emissions data from two tests are much higher than previously reported, the median of the $PM_{2.5}$ mass EFs we measured from four coal briquette stoves in China (5.5 g/kg-fuel) is comparable to the average $PM_{2.5}$ emission factor of 5.2 ± 0.5 g/kg-fuel for four Chinese coal briquette-burning stoves measured by Zhang et al. (2008).

The charcoal stoves from Uganda had the lowest $PM_{2.5}$ mass EFs, with a median of 1.7 g/kg-fuel (IQR: 2.0 g/kg-fuel). Previous estimates of $PM_{2.5}$ emissions from uncontrolled cooking with charcoal stoves in East Africa ranged from 1.0 to 23.4 g/kg with a mean of 6.3 kg (Johnson et al., 2014), substantially higher than the emission factors presented here. The disparity may be due to differences between startup versus hot operation emissions. Laboratory testing with charcoal stoves have found very high startup emissions, but much lower emissions once the stove is warm (Jetter and Kariher, 2009). Our tests, which had a median length of 168 min in Uganda, were longer than previous field tests of charcoal stoves in East Africa (18–112 min (Johnson et al., 2014),) which reduces the contribution of startup to the test-average emissions. Our measured $PM_{2.5}$ emissions from charcoal stoves fall within the wide range reported in the literature for laboratory tests: between 0.12 and 4.11 g/kg-fuel (Edwards et al., 2014).

$PM_{2.5}$ EFs in India and Honduras (wood) were similar, and fell between those of China (coal) and Uganda (charcoal). The median $PM_{2.5}$ mass EFs was 3.7 g/kg-fuel (IQR: 3.03 g/kg-fuel) in India and 4.1 g/kg-fuel (IQR of 3.2 g/kg-fuel) in Honduras. The emissions measured in this study in Honduras were more than a factor of two lower than those measured by Roden et al. in Honduras (8.5 ± 1.6 g/kg-fuel (Roden et al., 2006)). We performed a similar number of tests on similar stove technologies/operations, though their measurements included startup events.

The OC:EC ratio of $PM_{2.5}$ is an indicator of the potential climate impact (Kodros et al., 2015). A larger ratio likely indicates a higher

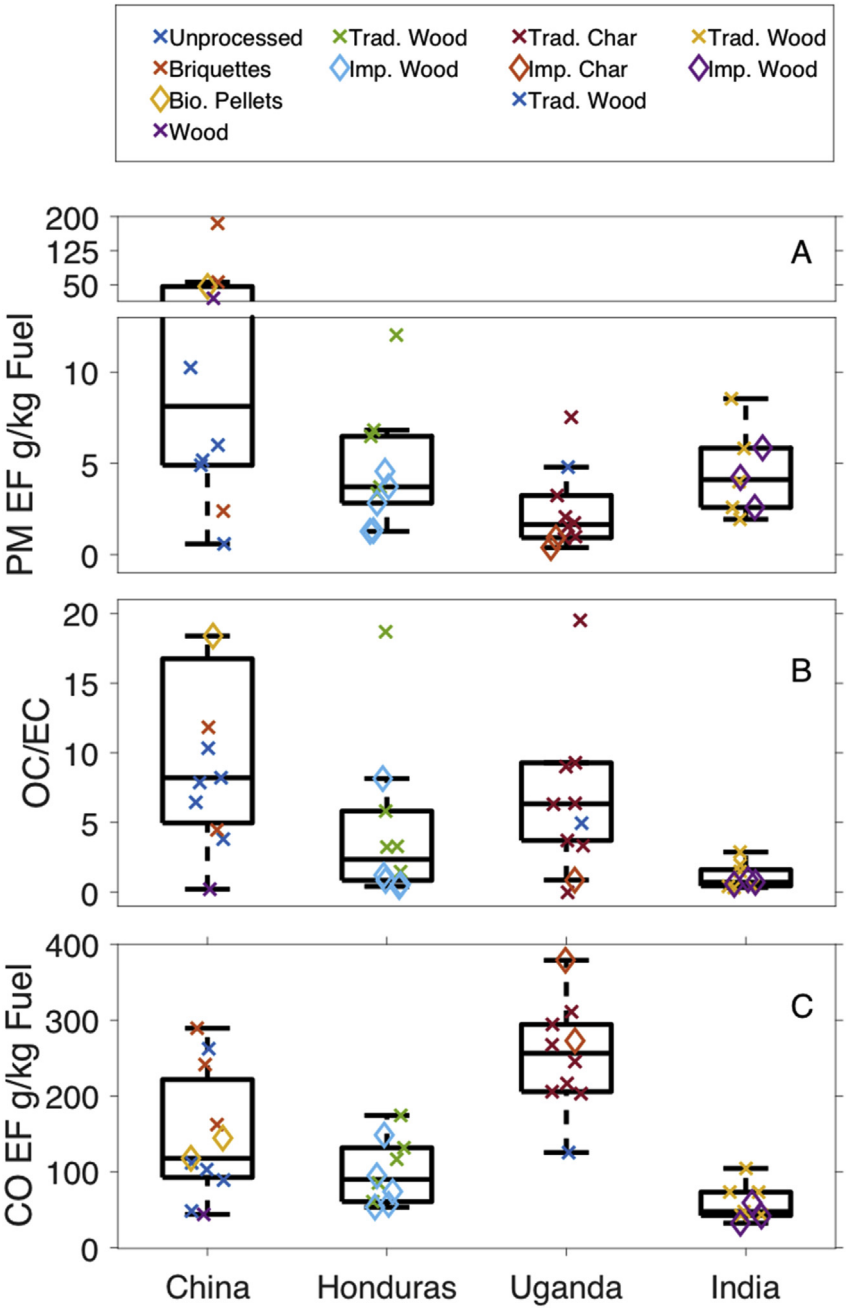

Fig. 2. Box whisker plots a) fine particulate matter (PM2.5) emission factors (EFs) b) Organic-carbon-to-elemental-carbon (OC:EC) ratios and c) Carbon monoxide (CO) EFs by country. Note the broken y-axis scale in (a). The central lines indicate the median, and the top and bottom of the boxes indicate the 75th and 25th percentiles. The whiskers extend to the most extreme data points not considered outliers.

light scattering fraction of PM (assuming non-absorbing OC) while a smaller ratio indicates a higher light absorption fraction of PM. Given that light scattering PM may lead to net climate cooling and light absorbing PM leads to net climate warming, this fraction may be an indicator of the net direction of climate impacts. Like gravimetric $PM_{2.5}$ mass, the ratio of OC:EC ratio was variable and positively skewed, with the data ranging from 0.2 to 120. Fig. 2b shows the ratios for each country. The median OC:EC ratio was 3.8, with an interquartile range of 7.5 across all countries. We measured the smallest OC:EC ratios for wood stoves in India (median: 0.7, IQR: 1.0) indicating highly absorbing particles. Emissions from Honduran wood stoves had higher OC:EC ratios (median: 2.4, IQR: 4.2). Coal and charcoal stoves had large OC emissions compared to EC, with median ratios of 8.2 (IQR: 9.6) and 6.3 (IQR: 5.1), respectively.

Fig. 2c summarizes the test-average CO EFs by country. The median CO EF across all tests was 114 g/kg-fuel with a large interquartile range of 143.5 g/kg-fuel, reflecting substantial stove-to-stove variability driven by differences in stove operations, with smoldering operations emitting more CO (lower MCE). Chinese and Ugandan stoves emitted more CO than stoves in Honduras and India. Test-average CO EF of 256 g/kg-fuel (IQR: 81 g/kg-fuel) for stoves in Uganda and 117 g/kg-fuel (IQR: 79 g/kg-fuel) for stoves in China. The median CO EFs for wood stoves were lower: 47.4 g/kg-fuel (IQR: 30 g/kg-fuel) in India and 89.9 g/kg-fuel (IQR: 64 g/kg-fuel) in Honduras. We did not find any correlation ($R^2 = 0.002$) between test-average CO and $PM_{2.5}$ emission factors, consistent with other studies (Carter et al., 2017). There was, however, modest correlation ($R^2 = 0.6$) between the average CO and POA EFs for woodstoves in both India and Honduras.

Emissions from cookstoves are a function of both fuel type and the combustion conditions. For complete combustion, volatile fuel needs sufficient residence time at high oxygen and temperature. Insufficient fuel surface area, poor mixing, or contact with relatively cold surfaces (such as the surface of a pot) can lead to pollutant formation. Fuel properties can also contribute to increased formation of PM. For example, fuel moisture can lead to lower flame temperatures and, coal can contain impurities such as nitrogen, sulfur, and ash (Edwards et al., 2014).

Wood was the primary fuel in both Honduras and India. Therefore, comparing the data from these two countries provides insight into the effects of stove technology (planchas vs. mud chulhas and ceramic stoves) and cooking practices on emissions, while holding the fuel category, wood, constant. The overall $PM_{2.5}$ emission rates of Honduran and Indian wood stoves are similar, but Indian stoves have higher EC emissions (and therefore lower OC:EC ratio). Fig. 2b indicates that, while $PM_{2.5}$ mass EFs for wood stoves in Honduras and India were similar, there were important differences in $PM_{2.5}$ composition. The emissions in India were more absorbing than those in Honduras: EC contributed a much larger fraction of the $PM_{2.5}$ emissions in India (OC:EC median 0.7, IQR: 1.0) than in Honduras (OC:EC median: 2.4, IQR: 4.2). OC:EC ratios depend on the combustion phase, which depends on cooking styles: a smoldering fire, with lower temperatures, likely emits more OC, while EC formation requires high temperature flaming combustion to form (Roden et al., 2006; Bond, Doherty and Fahey, 2013). Consistent with previous studies, Fig. S4 indicates that the test-integrated OC:EC ratio decreases with MCE. In India, cooking involved shorter cooking times likely with more flaming events compared to Honduras. These conditions resulted in higher EC EFs in India (0.76 g/kg-fuel [IQR 0.48 g/kg-fuel] than Honduras (0.51 g/kg-fuel [IQR 0.32 g/kg-fuel]) as well as significantly smaller CO EFs in India than in Honduras ($p = 0.01$).

Currently, it is unclear whether "improved" stoves will substantially lower emissions (Roden et al., 2009). Fig. 3a–c compares emissions for all wood-burning "improved" and traditional cookstoves. There was not a statistically significant difference in $PM_{2.5}$ emission factors between traditional and the rocket stoves in India. However, we did measure slightly lower $PM_{2.5}$ emission factors in Honduran "improved" plancha stoves compared to their traditional counterparts, but the differences were not statistically significant (possibly due to small sample size). Previous studies have reported lower $PM_{2.5}$ emissions in similar types of "improved" stoves compared to traditional stoves in Honduras (Johnson et al., 2008), no differences between "improved" and traditional stoves in Uganda (Johnson et al., 2011), and worse performance of natural draft rocket compared to traditional stoves in India (Kar et al., 2012). The OC:EC ratios of "improved" stoves were smaller than traditional ones. This could be due to the fact that many "improved" stoves are designed to improve thermal efficiency, which often leads to higher combustion temperatures and likely more EC production.

Climate impacts of cookstove emissions depend in part on the particle size distributions of the emissions (Kodros et al., 2015), which have been measured under controlled conditions (Li et al., 2009; Li et al., 2007; Arora et al., 2013; Just et al., 2013), but not during normal stove use events in homes, to our knowledge. Fig. 4 presents measured particle number distributions by country. The median GMD of Chinese stoves was 66 nm with an IQR of 51 nm (three individual tests with very high $PM_{2.5}$ EFs had much higher average median diameters of 149, 123, and 126 nm). In Honduras, the median test-average particle diameter was 48 nm, with relatively little test-to-test variability (IQR 7.8 nm). The Ugandan number size distribution had a median GMD of 39 nm (IQR: 14 nm). When all Ugandan tests were averaged, the distribution appears tri-modal, with modes near 15, 30, and 100 nm. The peaks at smaller diameters suggest that there could be nucleation of organic gases in the exhaust of the charcoal stoves, due to lower combustion temperature. The Indian wood stoves emissions had a median GMD of 76 nm and an IQR of 22 nm.

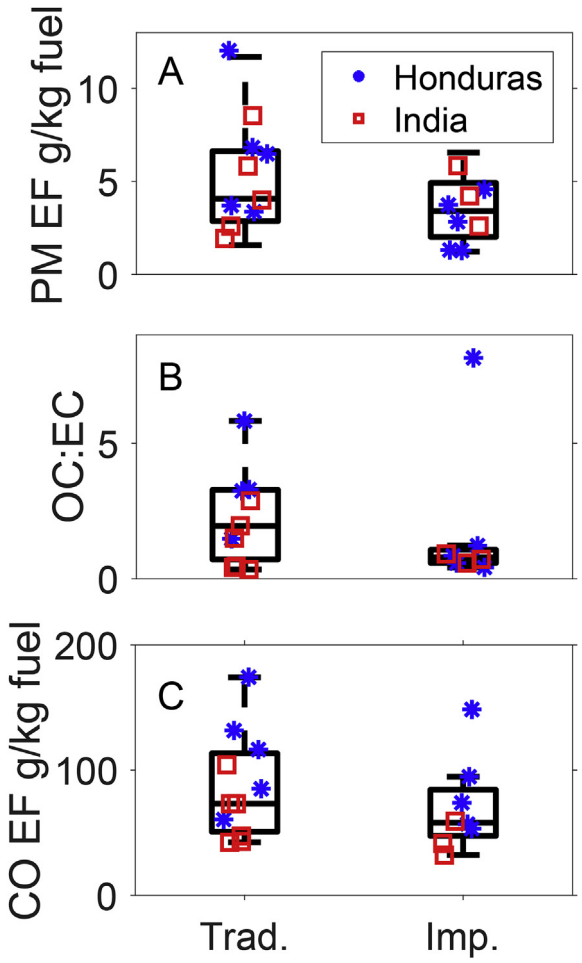

Fig. 3. Box whisker plots of a) fine particulate matter (PM2.5) emission factors (EFs) b) Organic carbon-to-elemental-carbon (OC:EC) ratios and c) carbon monoxide (CO) EFs for traditional vs. "improved" woodstoves. The underlying individual data points are also shown. The total PM2.5 EFs in Honduras and India were quite similar (p = 0.9). The differences between "improved" and traditional stoves are not statistically significant. The central lines indicate the median, and the top and bottom of the boxes indicate the 75th and 25th percentiles. The whiskers extend to the most extreme data points not considered outliers.

The total particle number (PN) EFs for the measured range (10 nm–420 nm) for China, Uganda, and India are plotted in Fig. 4b. We do not report PN EFs from Honduras due to SMPS flow errors during testing. The country-average total PN EFs varied by two orders of magnitude. On average, the PN emission factors were an order of magnitude higher for stoves in China than in Uganda, which were, in turn, an order of magnitude greater than for stoves in India.

The measured particle size distributions have a somewhat smaller mode than distributions used by emission inventories for climate models, and vary between regions. Most current emissions inventories only provide total mass emission rates, and hence, users of these inventories generally assume a uniform particle size distribution. Aerosol effects in climate models are, however, sensitive to differences in size; regional variability in size will change the spatial distribution of DRE and AIE estimates relative to previous studies (Kodros et al., 2015).

3.2. Real-time emissions

Fig. 5 shows a time series of measured pollutant emissions from a test in India, which illustrates the types of behavior across tests. Fig. 5a plots PN distributions as well as the total PN EF and the median particle

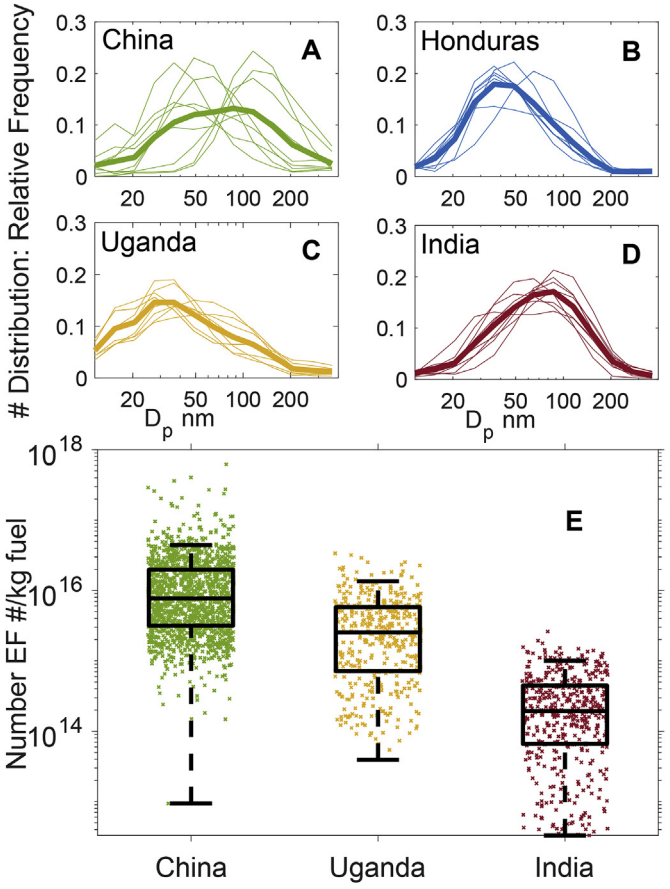

Fig. 4. A)-d): Average normalized particle number size distributions and (e) box-whisker plot of total number emission factors (EFs) for each country. We normalized the distribution in each scan by the total number concentration, then averaged over the test. In (e) note the log scale on the y-axis. The central lines indicate the median, and the top and bottom of the boxes indicate the 75th 25th percentiles. The whiskers extend to the most extreme data points not considered outliers. Total particle number (PN) EFs from Honduras were not included due to SMPS instrument errors during testing.

diameter for the measured range. A time series of the MCE and CO and BC EFs is plotted in Fig. 5b. EFs varied widely during the test, particularly BC and PN. Higher emissions often occurred at startup and when fuel was added during cooking. The size of the particles generated at startup, with a median around 150 nm, were also larger than those during the rest of the test, which had a median value of 94 nm.

The time series data give insight into relationship between different pollutants. In 6 out of the 10 tests in India, there were very high particle number emissions immediately after ignition, which corresponded to spikes in BC. This is visible in Fig. 5 at the beginning of the test. After ignition, it was more challenging to discern the association of emissions spikes and fueling events during cooking in India, because cooks added fuel every one to 5 min. In China and Honduras, stoves were often operated continuously throughout the day, making it difficult to capture startup events; however, emissions spikes associated with individual fuel addition events were more discernable.

Fig. 5 demonstrates that increases in CO EF are not always associated with increases in PN EF. For example, the spike in CO EF just after ignition (5b) does correspond to high particle number and size (and high BC). However, during the smoldering combustion between events 5 and 6, there is a peak in the CO EF, but few particles and almost no BC emissions. There are also periods of high PN emissions when BC EF are low, such as 10 min into the test (between events 1 and 2), which suggests high POA emissions.

Total BC emissions were dominated by distinct high concentration events, similar to the results of Chen et al. (Chen Y. R., 2012), as can be seen in Fig. 5. The BC EF in almost every test had a low baseline with intermittent spikes. In comparison, CO emissions are much more evenly distributed across in time across the entire stove use period. In India, BC emissions were dominated by an emissions spike immediately after ignition, and in some cases one or two more spikes later in the testing period. The event-driven nature of BC emissions was particularly clear in the longer time series of Honduran cooking; there was a very clear spike in the BC emissions corresponding to each time the stove operator added fuel.

There was not a nucleation mode (< 40 nm) in test-average emissions (Fig. 4), except for in Uganda. However, Fig. 5 indicates that there are intermittent emissions of smaller particles. For example, Fig. 5 shows a nucleation mode between events 3 (fuel added) and 4 (fuel bed stirred, fuel added.) where a slight dip in the MCE corresponds to a peak

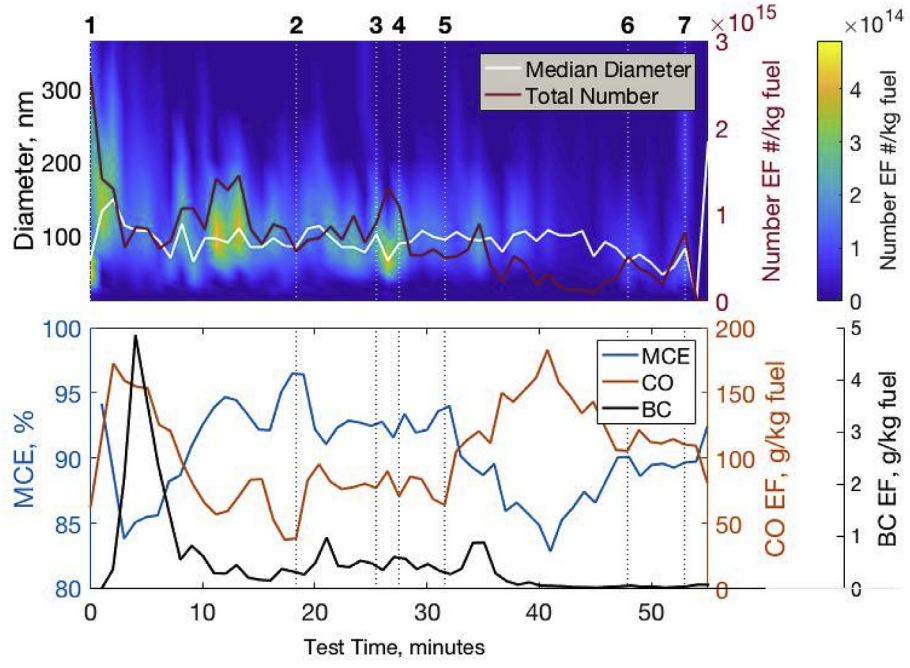

Fig. 5. Representative time series data from one test in India. a) Median particle diameter and total number concentration are superimposed on the real-time size distributions. b) modified combustion efficiency (MCE), and carbon monoxide (CO) and black carbon (BC) emissions factors (EFs). The numbers above the panel a) indicate cooking events: Event 1: Pot added. Event 2: fuel bed stirred, fuel added. Event 3: Fuel added. Event 4: fuel bed stirred, fuel added. Event 5: Fuel added. Event 6: fuel bed stirred, removed embers. Event 7: fuel bed stirred, removed embers.

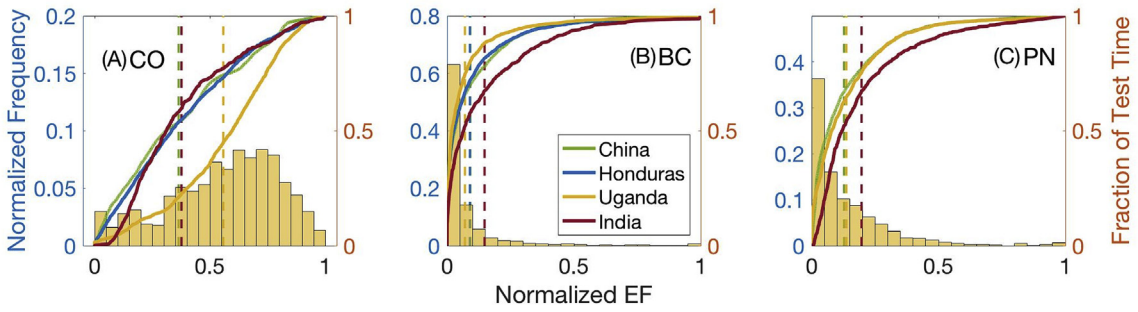

Fig. 6. Normalized histograms and empirical cumulative distribution functions (ECDFs) for (A) carbon monoxide (CO) (B) black carbon (BC) and (C) particle number (PN) emission factors (EFs). Histograms from Uganda were included to visually illustrate the distributions. The x-axes are normalized EF (normalized by the cumulative EF in each test.) 0.5 on the x-axes corresponds to the median EF. The left-hand y-axes are the normalized frequency, or the fraction of time the EF fell within a specified range of EFs. The right-hand y-axes represent the fraction of test time. These distributions therefore show what fraction of the emissions were emitted in what fraction of the test time. The vertical dashed lines are the normalized mean EF for each country, provided for reference.

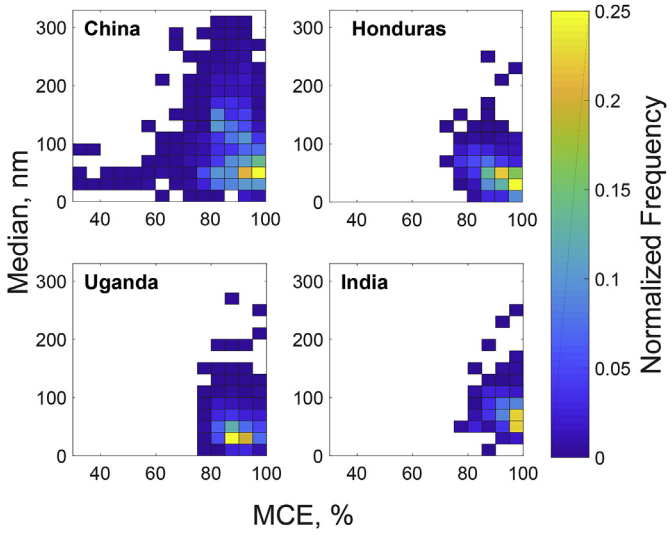

Fig. 7. Bivariate histograms comparing the frequency and distribution of modified combustion efficiency (MCE) and mode of particle number size distribution for all tests grouped by country. The colors represent normalized frequency, or the fraction of time the MCE and median particle size fell within a bin.

in the total number and a reduction in the median diameter.

We plotted the distributions of real-time emissions and stove operations (MCE) data in Figs. 6 and 7 to quantify the importance of emission events. Fig. 6 shows histograms and the empirical cumulative distribution functions of the measured CO, BC, and PN EFs. Fig. 7 shows bivariate distributions of particle number and MCE distributions.

Skewness quantifies the asymmetry of a distribution about the mean. A perfectly symmetric distribution has a skewness of zero, while a positive value indicates the contributions of high emission events.

To compare distribution of emissions between tests, we normalized the distributions in Fig. 6 by the cumulative emissions and the test length. Therefore, the x-axis indicates the fraction of total emissions, and the right y-axis indicates the fraction of test time; both axes vary from zero to one. A value of 0.5 on the x-axis corresponds to the median EF. The left-side y-axis, associated with the histograms, represents the normalized frequency, or the fraction of time that emission factors were within the given bin.

For every country, Fig. 6 demonstrates that the BC emissions are highly positively skewed, with an average skewness of 3.0. This high skewness indicates that in essentially every test, the overall BC emissions are driven by a relatively small number of high-emission events, as illustrated in the time series in Fig. 5b. These high-emission events often corresponded to startup or fuel addition events. If emissions are event-driven (positively skewed) then a stove designer could focus on those operations to reduce overall emissions. CO emissions are, in comparison to BC, relatively evenly distributed across the entire test, with an average skewness of 0.30, again consistent with the time series data in Fig. 5. The particle number EF was slightly less skewed than the BC, though still much more so than the CO EF (average skewness of 2.2).

Fig. 7 indicates that stoves in China were operated over the widest range of MCEs, dropping as low as 50%. The MCE in China is far from a normal distribution. As can also be seen in Fig. 7, particle size in China is highly variable, modestly skewed towards high MCEs and smaller particle sizes. Much larger particle sizes were observed in China than in other countries. The MCE distributions in Uganda and Honduras are similar and both close to normal with modes near 90%. India had the narrowest range of MCE values. Because different combustion conditions change the characteristic of a stove's emissions, time-resolved measurements of MCE can be used to inform laboratory protocols to produce more representative results.

4. Conclusions

Field measurements of emissions from solid fuel-burning stoves are challenging to collect but critical for establishing credible inventories of real-world emissions. Our data demonstrate the variability of emissions between different regions and between individual stoves.

The highest $PM_{2.5}$ mass emissions were observed in China. The positively skewed nature of the distribution of emissions measured in the field makes it difficult to quantify robust averages because they are sensitive to the frequency of high emitters. We found several homes in China with “superemitter” stoves: those with $PM_{2.5}$ EFs 5–20 times greater than the median value. The concept of “superemitters” has been seen in the vehicle fleet (Park et al., 2011) and the natural gas system (Mitchell et al., 2015). Locating homes with superemitting stoves and reducing their emissions could provide a cost-effective strategy for mitigating overall emissions.

Charcoal-burning stoves in Uganda had the lowest $PM_{2.5}$ EFs, however, this analysis does not capture the emissions generated during charcoal production, which can be important.

Real-time emissions and operations data reveal that certain operation modes can lead to high emissions; both BC and PN emissions were driven by high emission events. This result could inform stove design: by focusing on reducing emissions in those operational modes that lead to the highest emissions, the overall emissions could be greatly reduced. Because different combustion conditions change the characteristic of a stove's emissions, the distribution of MCEs from uncontrolled cooking in the field could be a useful tool for laboratory studies to ensure that a representative range of operating conditions is tested.

Our data from wood-burning stoves in India and Honduras illustrate

how differences in cooking styles and stove design, not just fuel type, influence emissions. Although the $PM_{2.5}$ mass EFs in both countries were similar, the shorter higher intensity cooking events with flaming combustion in India caused higher EC emissions compared to the longer, more smoldering cooking fire in Honduras.

Similar fuel-based emission factors were found between "improved" and traditional stoves, with the "improved" stoves tested here likely not providing substantive emissions reductions. However, we recognize that fuel-based emissions factors are an imperfect metric for comparing traditional and "improved" cookstoves, as they do not capture the potential of improved stoves to lower fuel consumption due to the increased thermal efficiency, which would lead to reduced cumulative emissions per cooking event.

To the best of our knowledge, we also report the first cookstove source size distributions measurements from uncontrolled in-home use events, an important input for simulations of aerosol climate impacts. Currently, emissions inventories generally just include mass of emissions based on stove and fuel variability, but do not include information about the size distribution. We found that particle size distributions are regionally dependent, and therefore should not be treated as uniform when being used as inputs in global models. While near-source coagulation may reduce differences in size distributions between stoves, the initial size distributions still matter (Sakamoto et al., 2016). Variability in size distributions between regions will change the spatial distribution of radiative effects relative to previous estimates (Kodros et al., 2015). In the future, more region-specific data are needed for climate modelers to improve their estimates of the DRE and AIE.

Acknowledgements

This research was supported by the U.S. Environmental Protection Agency STAR program under Assistance Agreement No. 835438. It has not been formally reviewed by EPA. The views expressed in this document are solely those of authors and do not necessarily reflect those of the Agency. EPA does not endorse any products or commercial services mentioned in this publication. We thank our local partners: Department of Building Technology and Science, School of Architecture, Tsinghua University in Beijing, China; The Center for Research in Energy and Energy Conversion in Makerere University, Kampala, Uganda; and Faculty of Public Health, Sri Ramachandra Medical College and Research Institute, Chennai, India. We thank Andy Grieshop for sharing information on his sampler design. Finally, we are extremely grateful to the participants who graciously allowed us into their homes to conduct the fieldwork.

Appendix A. Supplementary data

Supplementary data related to this article can be found at https://doi.org/10.1016/j.atmosenv.2018.06.041.

References

Adkins, E.T., 2010. Field testing and survey evaluation of household biomass cookstoves in rural sub-Saharan Africa. Energy.Sustain. Dev. 14 (3), 172–185.
Arora, P., Jain, S., Sachdeva, K., 2013. Physical characterization of particulate matter emitted from wood combustion in improved and traditional cookstoves. Energy.Sustain. Dev. 17 (5), 497–503.
Bailis, R., Berrueta, V., Chengappa, C., Dutta, K., Edwards, R., Masera, O., Smith, K.R., 2007. Performance testing for monitoring improved biomass stove interventions: experiences of the Household Energy and Health Project. Energy.Sustain. Dev. 11 (2), 57–70.
Bhattacharya, S.C., Albina, D.O., Khaing, A.M., 2002. Effects of selected parameters on performance and emission of biomass-fired cookstoves. Biomass Bioenergy 23 (5), 387–395.
Bond, T.C., Streets, D.G., Yarber, K.F., Nelson, S.M., Woo, J.H., Klimont, Z., 2004. A technology-based global inventory of black and organic carbon emissions from combustion. J. Geophys. Res.: Atmosphere 109 (14), 1–43.
Bond, T., Doherty, S., Fahey, D., 2013, June;al.,. Bounding the role of black carbon in the climate system: a scientific assessment. J. Geophys. Res. Atmos. 118 (11), 5380–5552.
Carter, E., Norris, C., Dionisio, K.L., Balakrishnan, K., Checkley, W., Clark, M.L., Baumgartner, J., 2017. Assessing exposure to household air pollution: a systematic review and pooled analysis of carbon monoxide as a surrogate measure of particulate matter. Environ. Health Perspect. 125 (7), 1–12.
Chen, X.L., 2015. Pollutant emissions from improved coal- and wood-fuelled cookstoves in rural households. Environ. Sci. Technol. 49 (11), 6590–6598.
Chen, Y.R., 2012. Characterizing biofuel combustion with patterns of real-time emission data (PaRTED). Environ. Sci. Technol. 46 (11).
Chow, J.C., Watson, J.G., Chen, L.A., Chang, M.O., Robinson, N.F., Dana, T., Kohl, S., 2007. The IMPROVE_A temperature protocol for thermal/optical carbon analysis: maintaining consistency with a long-term database. J. Air Waste Manag. Assoc. 57 (9), 1014–1023.
Coffey, E.R., Muvandimwe, D., Hagar, Y., Wiedinmyer, C., Kanyomse, E., Piedrahita, R., Hannigan, M.P., 2017. New emission factors and efficiencies from in-field measurements of traditional and improved cookstoves and their potential implications. Environ. Sci. Technol. 51 (21), 578–583.
Dutta, K., Shields, K.N., Edwards, R., Smith, K.R., 2007. Impact of improved biomass cookstoves on indoor air quality near Pune, India. Energy.Sustain. Dev. 11 (2), 19–32.
Edwards, R., Karnani, S., Fisher, E.M., Johnson, M., Naeher, L., Smith, K.R., Morawska, L., 2014. WHO Indoor Air Quality Guidelines: Household Fuel Combustion. IAQ Guidlines. World Health Organization.
Ezzati, M., Kammen, D., 2001. Quantifying the effects of exposure to indoor air pollution from biomass combustion on acute respiratory infections n developing countries. Environ. Health Perspect. 109 (5), 481–488.
Ezzati, M., Mbinda, B.M., Kammen, D.M., 2000. Comparison of emissions and residential exposure from traditional and improved cookstoves in Kenya. Environ. Sci. Technol. 34 (4), 578–583.
Global Alliance for Clean Cookstoves, 2012, FebruaryGlobal Alliance for Clean Cookstoves,. IWA tiers of performance. In: International Workshop Agreement, International Organization for Standardization. The Haue, Netherlands.
Grieshop, A.P., Jain, G., Sethuraman, K., Marshall, J.D., 2017. Emission factors of health- and climate-relevant pollutants measured in home during a carbon-finance-approved cookstove intervention in rural India. GeoHealth 1 (5), 222–236.
Hagler, G.S., Yelverton, T.L., Vedantham, R., Hansen, A.D., Turner, J.R., 2011. Post-processing method to reduce noise while preserving high time resolution in aethalometer real-time black carbon data. Aerosol Air Qual. Res. 11 (5), 539–546.
Hu, W.W., Hu, M., Yuan, B., Jimenez, J.L., Tang, Q., Peng, J.F., He, L.Y., 2013. Insights on organic aerosol aging and the influence of coal combustion at a regional receptor site of central eastern China. Atmos. Chem. Phys. 13 (19), 10095–10112.
Jetter, J., Kariher, P., 2009. Solid-fuel household cook stoves: characterization of performance and emissions. Biomass Bioenergy 33 (2), 294–305.
Johnson, M., Edwards, R., Frenk, C.A., Masera, O., 2008. In-field greenhouse gas emissions from cookstoves in rural Mexican households. Atmos. Environ. 42 (5), 1206–1222.
Johnson, M., Garland, C., Jagoe, K., Pennise, D., Charron, D., Scott, P., Khoi, D., 2014. Cookstove Emissions Performance Survey. Technical Report. Global Alliance for Clean Cookstoves, Washington DC.
Johnson, M., Lam, N., Pennise, D., Charron, D., Bond, T., Modi, V., Ndemere, J.A., 2011. In-Home Emissions of Greenhouse Pollutants from Rocket and Traditional Biomass Cooking Stoves in Uganda. USAID. USAID.
Just, B., Rogak, S., Kandlikar, M., 2013. Characterization of ultrafine particulate matter from traditional and improved biomass cookstoves. Environ. Sci. Technol. 47 (7), 3506–3512.
Kar, A., Rehman, I., Burney, J., Puppala, S.P., Suresh, R., Singh, L., Ramanathan, V., 2012. Real-time assessment of black carbon pollution in indian households due to traditional and improved biomass cookstoves. Environ. Sci. Technol. 46 (5), 2993–3000.
Kirchstetter, T.W., Novakov, T., 2007. Controlled generation of black carbon particles from a diffusion flame and applications in evaluating black carbon measurement methods. Atmos. Environ. 41 (9), 1874–1888.
Koch, D., Bond, T.C., Streets, D., Unger, N., Werf, G.R., 2007. Global impacts of aerosols from particular source regions and sectors. J. Geophys. Res.: Atmosphere 112 (D2), 1–24.
Kodros, J.K., Scott, C.E., Farina, S.C., Lee, Y.H., L'Orange, C., Volckens, J., Pierce, J.R., 2015. Uncertainties in global aerosols and climate effects due to biofuel emissions. J. Atmos. Chem. Phys. 15 (15), 8577–8596.
Kodros, J., Carter, E., Brauer, M., Volckens, J., Bilsback, K., L'Orange, C., Pierce, J., 2018. Quantifying the contribution to uncertainty in mortality attributed to household, ambient, and joint exposure to PM2. 5 from residential solid fuel use. GeoHealth 2 (1), 25–39.
Lacey, F., Henze, D., 2015. Global climate impacts of country-level primary carbonaceous aerosol from solid-fuel cookstove emissions. Environ. Res. Lett. 10.
Leavey, A.L., 2015. Real-time particulate and CO concentrations from cookstoves in rural households in udaipur, India. Environ. Sci. Technol. 49 (12), 7423–7431.
Li, X., Duan, L., Wang, S., Duan, J., Guo, X., Yi, H., Hao, J., 2007. Emission characteristics of particulate matter from rural household biofuel combustion in China. Energy Fuel. 21 (2), 845–851.
Li, X., Wang, S., Duan, L., Hao, J., Nie, Y., 2009. Carbonaceous aerosol emissions from household biofuel combustion in China. Environ. Sci. Technol. 43 (15), 6076–6081.
MacCarty, N., Ogle, D., Still, D., Bond, T., Roden, C., 2008. A laboratory comparison of the global warming impact of five major types of biomass cooking stoves. Energy.Sustain. Dev. 12 (2), 56–65.
Masera, O., Edwards, R., Arnez, C.A., Berrueta, V., Johnson, M., Bracho, L.R., Smith, K.R., 2007. Impact of Patsari improved cookstoves on indoor air quality in Michoacán, Mexico. Energy.Sustain. Dev. 11 (2), 45–56.
Mitchell, A.L., Tkacik, D.S., Roscioli, J.R., Herndon, S.C., Yacovitch, T.I., Martinez, D.M.,

Robinson, A.L., 2015. Measurements of methane emissions from natural gas gathering facilities and processing plants: measurement results. Environ. Sci. Technol. 49 (5), 3219–3227.
Park, S.S., Kozawa, K., Fruin, S., Mara, S., Hsu, Y.-K., Jakober, C., Herner, J., 2011. Emission factors for high-emitting vehicles based on on-road measurements of individual vehicle exhaust with a mobile measurement platform. J. Air Waste Manag. Assoc. 61 (10), 1046–1056.
Roden, C.A., Bond, T.C., Conway, S., Pinel, A.B., 2006. Emission factors and real-time optical propertiesof particles emitted from traditional wood burning cookstoves. Environ. Sci. Technol. 40 (21), 6750–6757.
Roden, C.A., Bond, T.C., Conway, S., Pinel, A.B., MacCarty, N., Still, D., 2009. Laboratory and field investigations of particulate and carbon monoxide emissions from traditional and improved cookstoves. Atmos. Environ. 43 (6), 1170–1181.
Sakamoto, K.M., Laing, J.R., Stevens, R.G., Jaffe, D.A., Pierce, J.R., 2016. The evolution of biomass-burning aerosol size distributions due to coagulation: dependence on fire and meteorological details and parameterization. Atmos. Chem. Phys. 16, 7709–7724.
Shen, G., Chen, Y., Xue, C., Lin, N., Huang, Y., Shen, H., Tao, S., 2015. Pollutant emissions from improved coal- and wood-fuelled cookstoves in rural households. Environ. Sci. Technol. 49 (11), 6590–6598.
Spliethoff, H., 2010. Solid Fuels. In Power Generation from Solid Fuels, 1 ed. Springer-Verlag, Berlin Heidelberg.
Subramanian, R., Khlystov, A.Y., Cabada, J.C., Robinson, A.L., 2004. Positive and negative artifacts in particulate organic carbon measurements with denuded and undenuded sampler configuration. Aerosol. Sci. Technol. 38 (S1), 27–48.
Turpin, B.J., Lim, H.-J., 2001, FebruaryTurpin and Lim,. Species contributions to PM2.5 mass concentrations: revisiting common assumptions for estimating organic mass. Aerosol. Sci. Technol. 35 (1), 602–610.
Wathore, R., Mortimer, K., Grieshop, A.P., 2017. In-use emissions and estimated impacts of traditional, natural- and forced-draft cookstoves in rural Malawi. Environ. Sci. Technol. 51 (3), 1929–1938.
Wei, S., Shen, G., Zhang, Y., Xue, M., Xie, H., Lin, P., Tao, S., 2014. Field measurement on the emissions of PM, OC, EC and PAHs from indoor crop straw burning in rural China. Environ. Pollut. 184, 18–24.
World Health Organization, May 8th, 2018. Household Air Pollution and Health Fact Sheet. http://www.who.int/en/news-room/fact-sheets/detail/household-air-pollution-and-health.
Zhang, J., Smith, K.R., Ma, Y., Ye, S., Jiang, F., Qi, W., Thorneloe, S.A., 2000. Greenhouse gases and other airborne pollutants from household stoves in China: a database for emission factors. Atmos. Environ. 34 (26), 4537–4549.
Zhang, Y., Schauer, J.J., Zhang, Y., Zeng, L., Wei, Y., Liu, Y., Shao, M., 2008. Characteristics of particulate carbon emissions from real-world Chinese coal combustion. Environ. Sci. Technol. 42 (14), 5068–5073.